

# Graph embeddings via matrix factorization for link prediction: smoothing or truncating negatives?

Asan Agibetov<sup>a,\*</sup>

<sup>a</sup>*Section for Artificial Intelligence and Decision Support, Medical University of Vienna, Vienna 1090, Austria*

---

## Abstract

Link prediction – the process of uncovering missing links in a complex network – is an important problem in information sciences, with applications ranging from social sciences to molecular biology. Recent advances in neural graph embeddings have proposed an end-to-end way of learning latent vector representations of nodes, with successful application in link prediction tasks. Yet, our understanding of the internal mechanisms of such approaches has been rather limited, and only very recently we have witnessed the development of a very compelling connection to the mature matrix factorization theory. In this work, we make an important contribution to our understanding of the interplay between the skip-gram powered neural graph embedding algorithms and the matrix factorization via SVD. In particular, we show that the link prediction accuracy of graph embeddings strongly depends on the transformations of the original graph co-occurrence matrix that they decompose, sometimes resulting in staggering boosts of accuracy performance on link prediction tasks. Our improved approach to learning low-rank factorization embeddings that incorporate information from unlikely pairs of nodes yields results on par with the state-of-the-art link prediction performance achieved by a complex neural graph embedding model.

*Keywords:* graph embeddings; random walks; matrix factorization; information theory; link prediction

---

## 1. Introduction

In information sciences, networks are a convenient representation of the relationships of complex system components, such that the interconnectivity of nodes and edges inherently encodes valuable information about the system. It is such a flexible tool that has been used to represent complex emerging patterns in disparate domains, such as molecular biology and social sciences. Perhaps, one reason for the flexibility of this representation, is that the information stored within can be understood through the analysis of its topology. Since decades a very popular problem in information sciences has been the link prediction [7]. Which links are likely to emerge as a complex process unfolds? Given the current topology of the network, what are the missing links that we need to uncover? To address this problem, one common way is to treat the network as a graph  $G = (V, E)$  with nodes  $u \in V$  and edges  $(u, v) \in E; u, v \in V$ . Then, to perform link prediction, one would split the graph edges  $E$  into two partitions (not necessarily of the same size)  $E_{train}, E_{test}$ , which serve the purpose of *positive* edges. Next, we sample the non-existent edges  $(u, v) \notin E$  to make  $E_{train}^-, E_{test}^-$ , which serve as *negative* examples. Habitually, one would then come up with a prediction model that would learn patterns from the training dataset; typically learn to score positive edges higher than negatives. And the prediction performance of such a model would be assessed on the test set with an accuracy metric. As a result, one would hope that through this partitioning the prediction model would generalize enough to predict the future states of the system, i.e., to predict the formation of new links.

The conventional way to efficiently process the network structure to draw conclusions about the complex system relies on explicit topological descriptors, such as betweenness centrality and triangle count. The

---

\*Corresponding author; Währinger Strasse 25A, OG1.06, Vienna 1090, Austria  
*Email address:* asan.agibetov@meduniwien.ac.at (Asan Agibetov)

accuracy of such ad-hoc descriptors is directly proportionate to the expertise and domain-knowledge put into their design. However, recently, the field of representation learning has proposed a more flexible approach of learning latent representation of networks, which embeds the graph structure into a latent space. More specifically, given a graph  $G$  the goal is to learn a dictionary mapping  $V \mapsto \mathbb{R}^d$  that embeds each vertex to a  $d$ -dimensional vector. The link prediction is then performed by a classifier ( $V \times V \mapsto \mathbb{R}$ ) that for a pair of input vertices  $u, v$  scores the likelihood of them being connected (i.e., likelihood to form a link).

The roots of this line of work can be rooted back to the spectral graph theory [2] and social dimensional learning [14]. However, the more recent approaches (e.g., *deepwalk* [11], *node2vec* [4]) have been based on word embedding algorithms, in particular the skip-gram with negative sampling (SGNS) version of the *word2vec* model [10]. The central idea is that the node sequences  $w_1, w_2, \dots, w_n$  generated from random walks simulation on graphs can be treated as a text corpus and inputted into the word2vec model to get the output in a form of latent vector representation for each node (technically a word in the random walks generated text). While deepwalk-inspired approaches have been demonstrated to be effective in link prediction problems, their theoretical mechanisms have been relatively understudied, up until Qiu et al. [12] have explicitly demonstrated the connection of deepwalk-inspired approaches and matrix factorization methods. The central idea relies on the fact that the horseback of these approaches – word2vec – has been shown to implicitly factorize the matrix containing the collocation of words in the text. Concretely, Levy et al [6] have formally demonstrated that the word2vec is factorizing the point-wise mutual information (PMI) matrix - a well-known matrix in the information theory. Based on this demonstration, Qiu et al. [12] have given closed-form expressions for the PMI matrix that deepwalk-inspired methods are factorizing in graph-theoretic terms. This expression of the PMI matrix is dubbed the *deepwalk matrix* and its closed-form derivation is tightly connected to random walks and graph Laplacians. Finally, the authors proposed the netmf algorithm that learns network embeddings for nodes by performing the singular value decomposition (SVD) of the deepwalk matrix.

An important observation in this general approach to low-rank approximation of the PMI matrix is that this matrix may pose computational issues. The trouble kicks in when we have a pair of words  $(w, c)$  which are never observed ( $\#(w, c) = 0$ ). These *negative* pairs lead to the ill-posed task of decomposing  $\text{PMI}(w, c) = \log 0 = -\infty$  entries. As noted in [6], solutions to these problems include a Dirichlet prior by adding a small “fake” count to the underlying counts matrix - smoothing thus negative entries, or truncating the PMI matrix, such that  $\text{PMI}(w, c) = 0$  for the unobserved pairs. Qiu et al. [12] use the latter, mainly because they want to leverage the fact that a truncated matrix is very sparse, and thus SVD is accelerated. However, by forcing zeroes into the matrix we ignore the information from most of the entries of the matrix, as PMI scores for low-frequency pairs of nodes will be indistinguishable from pairs of nodes that truly never appear in contexts. We will show that this may lead to a serious drop in performance on link prediction problems.

### 1.1. Contribution of this work

In this work, we extend the work of Qiu et al. [12] and propose a new approach to learning low-rank factorization embeddings that incorporate information from unlikely pairs of nodes. The contributions of our work may be summarized in these three bullet points:

- We apply smoothing to shifted PMI scores to enable a low-rank factorization of matrix entries that does not penalize low-frequency node pairs. We show that this correction may drastically improve accuracy.
- By considering different transformations of the PMI matrix, and by deriving matrix forms of the joint probability matrix, we can demonstrate superior link prediction performance. These results lead us to argue that the linguistic collocation metric (PMI) may not be the best metric for link prediction.
- Finally, we compare our results with the state-of-the-art accuracy scores from the approach of Abu-El-Haija et al [1], and conclude that our approach is on par. Their algorithm is using a stochastic (implicit) matrix factorization using neural networks, while ours is based on explicit SVD.

### 1.2. Organization of this manuscript

This manuscript is organized as follows: in Section 2 we will highlight the theoretical notions that are necessary for a fluid reading of our work; in Section 3 we will review the specific steps we took to evaluate our approach on link prediction tasks; Section 4 will cover our results; finally, we will close with a discussion section (Section 5).

## 2. Theory

To improve the self-contained reading of this manuscript, we briefly highlight the most salient parts of the required theoretical concepts. In particular, we present the word2vec [10] algorithm that is used to learn latent vector representations for words. In this manuscript, we only focus on a specific training mode of this neural embedding model that relies on skip-gram negative sampling (SGNS) [9]. Then, following the treatment of Levy et al. [6], we show the connection of SGNS word2vec to implicit factorization of the shifted pointwise mutual information (PMI) matrix. Next, we present the notation used for graphs and the specifics of random walks generation. Finally, we present the synthesis of the main results of Qiu et al. [12] that connect random walks-based graph embedding algorithms and SGNS word2vec. This synthesis will re-interpret the implicit PMI matrix factorization in graph-theoretic terms. The theory reviewed in this section is necessary for a fluid presentation of our main results in this manuscript.

### 2.1. word2vec and connection to shifted pointwise mutual information

Word2vec [10] is an unsupervised neural embedding model that assigns a  $d$ -dimensional vector  $\vec{w} \in \mathbb{R}^d$  to every word  $w$  in a vocabulary  $V$ . The entries in the vectors are latent and treated as parameters to be learned. Word2vec model is usually trained using the negative-sampling procedure [9]. This particular way of training a neural model is referred to in the literature as skip-gram with negative sampling (SGNS). Full derivations of the model are available in [3].

In practice, the skip-gram model assumes a corpus of words  $w \in V_w$  and their contexts  $c \in V_c$ , where  $V_w$  and  $V_c$  are the word and context vocabularies. The words come from an unannotated textual corpus of words  $w_1, w_2, \dots, w_n$  ( $n \sim 10^9$ ) and the contexts for word  $w_i$  are the words surrounding it in an  $T$ -sized window  $w_{i-T}, \dots, w_{i-1}, w_{i+1}, \dots, w_{i+T}$ . The collection of observed words and context pairs  $(w, c)$  is denoted as a multiset  $\Omega$ ; multiset captures the fact that there will be multiple instances of one fixed pair  $(w_0, c_0)$ . This notation allows us to count frequencies of pairs of words  $\#(w, c)$  as they appear in  $\Omega$ , and derive marginal frequencies for individual words and contexts, with  $\#(w) = \sum_{c \in V_c} \#(w, c)$  and  $\#(c) = \sum_{w \in V_w} \#(w, c)$ , respectively.

The negative sampling objective aims to maximize  $P((w, c) \in \Omega | w, c)$  for observed pair  $(w, c)$  while maximizing  $P((w, c) \notin \Omega | w, c)$  for  $b$  randomly sampled “negative” examples. For a single observation the SGNS objective is defined as:

$$\log \sigma(\vec{w}, \vec{c}) + b \cdot \mathbb{E}_{c' \sim P_d} \left[ \log \sigma(-\vec{w} \cdot \vec{c}') \right],$$

where  $\sigma(x) = \frac{1}{1+e^{-x}}$  is the sigmoid function, and a negative context word  $c'$  is sampled according to an empirical unigram distribution  $P_\Omega(c) = \frac{\#(c)}{|\Omega|}$ . This objective is trained using the stochastic gradient descent. The global objective sums over all observed pairs in the corpus, as in

$$L_{\text{SGNS}} = \sum_{w \in V_w} \sum_{c \in V_c} \#(w, c) \left[ \log \sigma(\vec{w} \cdot \vec{c}) + b \cdot \mathbb{E}_{c' \sim P_d} \left[ \log \sigma(-\vec{w} \cdot \vec{c}') \right] \right].$$

SGNS embeds both words and their contexts into a low-dimensional space  $\mathbb{R}^d$ , resulting in word and context matrices  $W$  and  $C$ . Usually, the rows of the matrix  $W$  are typically used in NLP tasks while  $C$  is ignored. However, as Levy et al. [6] have pointed out, if we consider the product  $W \cdot C^T = M$ , then SGNS can be considered as an implicit factorization of the matrix  $M$  into two smaller matrices  $(W, C)$ . They formally showed that an entry  $M_{ij}$  in this matrix corresponds to a shifted pointwise mutual information

(PMI), which when applied to NLP measures the degree of the “collocation” between the word  $w_i$  and the context  $c_j$  (see Section 5 for more details). Concretely, for one word, context pair  $(w_i, c_j)$ , and for  $b$  negative samples, SGNS factorizes a matrix  $M$  whose  $ij$ -th entry equals

$$M_{ij} = \vec{w}_i \cdot \vec{c}_j = \log \left( \frac{\#(w, c)|\Omega|}{\#(w) \cdot \#(c)} \right) - \log b = \log \text{PMI} - \log b.$$

Note that, for a pair of discrete outcomes  $(x, y)$  the PMI metric computes the log of the ratio between their joint probability and their marginal probabilities. In practice, the probabilities are computed empirically, as in

$$\text{PMI}(x, y) = \log \frac{P(x, y)}{P(x)P(y)} = \log \left( \frac{\#(w, c)/|\Omega|}{\#(w)/|\Omega| \cdot \#(c)/|\Omega|} \right) = \log \left( \frac{\#(w, c)|\Omega|}{\#(w) \cdot \#(c)} \right).$$

As a last and very important note, Levy et al [6] warn that working with the PMI matrix presents computational challenges. In particular, the matrix  $M$  is ill-defined whenever we have pairs of words  $(w, c)$  which are never observed ( $\#(w, c) = 0$ ), since  $\text{PMI}(w, c) = \log 0 = \infty$ . Solutions to these problems include a Dirichlet prior by adding a small “fake” count to the underlying counts matrix or truncating the matrix  $M$ , such that  $\text{PMI}(w, c) = 0$  for the unobserved pairs. The former will produce a dense matrix, while the latter a sparse one. We will discuss this issue in detail in the discussion section of this manuscript.

## 2.2. Random walks on graphs

Following treatment of Lovász [8], let  $G = (V, E)$  be a connected graph with  $n$  nodes and  $m$  edges. Given a graph and a node  $u \in V$  as a starting point, we select a neighbor of  $u$  at random and move to this neighbor; then we select a neighbor of this point at random, and move to it, etc. The (random) sequence of points (nodes) selected this way is a *random walk* on a graph. Let  $A$  be the adjacency matrix of the graph  $G$ , such that  $A_{uv} = 1$  if nodes  $(u, v) \in E$  are connected, and  $A_{uv} = 0$  otherwise. We can compute the *degree* of each node  $d_u = \sum_i A_{ui}$  that indicates the number of neighbors for this node. It is possible to represent the degrees of all nodes of a graph  $G$  as a diagonal matrix  $D$ , with  $D_{ii} = d_i$ . The sum of all degrees in a graph is the *volume* of the graph, denoted as  $\text{vol}(G) = \sum_i d_i$ . Note that the inverse of  $D$  is  $D_{ii}^{-1} = 1/d_i$ .

Equipped with this terminology, we can formally represent the process of a random walk as follows in this section. Consider a probability distribution  $p_t$  that signals the position of a random surfer at the time  $t$ :

$$p_t(i) = \text{Prob}(v_t = i).$$

For instance,  $p_0$  could be the initial probability distribution from which we can sample the starting point of a random walk. We will transition to a neighbor of a starting point  $i$  with the probability

$$p_{ij} = \begin{cases} 1/d_i & \text{if } ij \in E, \\ 0 & \text{otherwise.} \end{cases}$$

Let  $P = D^{-1}A$  be the transition probability at step 1, then we can find the probability distribution of a random surfer at time  $t = 1$  with  $p_1^T = p_0^T P = p_0^T D^{-1}A$ . Even more conveniently, the  $ij$ -th entry of the matrix  $P^r = \underbrace{P \times \dots \times P}_{r \text{ times}}$  (repeated matrix multiplication) will give us the probability that we start at node  $i$  and in  $r$  steps of transition will end up in  $j$ .

Many network embedding algorithms rely on random walks for a corpus generation consisting of sequences of nodes  $w_1, w_2, \dots, w_n$ . These sequences are then processed by the word2vec [10] algorithm to learn low-dimensional vector representation (“embeddings”) of nodes of a graph  $G$ . We will present the necessary details of this process in the following subsections.

### 2.3. Matrix factorization, SVD and graph embeddings

Abu-El-Haija et al. [1] propose to view neural embeddings as a stochastic version of SVD applied to learn vector representations  $Y$  for the nodes of a graph  $G$ . They claim that the neural embedding methods essentially minimize the following loss function

$$\min_Y L(f(A), g(Y)),$$

where  $A$  is the adjacency matrix of a graph  $G$ ,  $f(\cdot)$  is some transformation of the adjacency matrix, and  $g : V \times V \mapsto \mathbb{R}$  is a pairwise edge function. For instance, a neural network can be trained to find a decomposition of  $A$  with two matrices  $L, R$  by minimizing the objective function

$$\min_{L,R} \|A - L \cdot R^T\|_F,$$

where  $f(A) = A$ ,  $g(Y) = L \cdot R^T$ , and  $\|\cdot\|_F$  is the Frobenius norm.

They also propose that the node2vec algorithm [4] can be seen under this framework by setting  $f(A) = C$ , where  $C$  is the co-occurrence matrix from random walks, such that each entry  $C_{uv}$  contain the number of times nodes  $v$  and  $u$  are co-visited within a context distance, in all simulated random walks. While these propositions have not been formally shown in [1], similar observations have been echoed by Qiu et al. [12], who approached the problem from the side of word embeddings. We detail this approach in the next section.

### 2.4. word2vec, deepwalk and PMI

Very loosely speaking, deepWalk [11] and the associated approaches, generate random walks  $w_1, w_2, \dots, w_n$  by starting from a random node sampled from a probability distribution [1]. These sequences of nodes are treated as sentences and passed to the word2vec algorithm to learn embedding representations for each node  $v$  in the graph  $G$ . In the case of graphs,  $\Omega$  consists of node pairs  $(w, c)$ . The interpretation of such a pair, as in the case of the word embeddings, is that a context node  $c$  occurs in the context window of size  $T$  around the node  $w$  (e.g.,  $c \in w_{i-T}, \dots, w_{i-1}, w_{i+1}, \dots, w_{i+T}$ ). Notice that we can count co-occurrence counts of two nodes  $\#(w, c)$  in any random walk, as in the case of word embeddings. In practice, one simulates  $L$  (e.g.,  $L = 80$ ) random walks per each node.

Due to their tight connection with word2vec and the associated SGNS loss, these methods are sometimes referred to as skip-gram powered network embedding methods [12]. Following the results of Levy et al. [6], Qiu et al. [12] have explicitly shown that the skip-gram powered network embedding methods (e.g., deepWalk [11], node2vec [4]), are in theory performing implicit matrix factorization. In particular, they connect the deepwalk’s implicit matrix and graph Laplacians, and propose the algorithm netmf to approximate the closed-form of the deepwalk’s implicit matrix. They start by formally showing that the co-occurrence probability term of the PMI could be re-interpreted in terms of transition probabilities on a graph, as in

$$\frac{\#(w, c)}{|\Omega|} \rightarrow_p \frac{1}{2T} \sum_{r=1}^T \left( \frac{d_w}{\text{vol}(G)} (P^r)_{w,c} + \frac{d_c}{\text{vol}(G)} (P^r)_{c,w} \right).$$

After a series of derivations, they finally propose the closed form of the shifted PMI matrix in terms of graph theory terminologies

$$\begin{aligned} M = \text{PMI} - \log b &= \log \left( \frac{\#(w, c) |\Omega|}{\#(w) \cdot \#(c)} \right) - \log b \\ &= \log \left( \frac{\text{vol}(G)}{T} \left( \sum_{r=1}^T (P^r) \right) D^{-1} \right) - \log b \\ &= \log \left( \frac{\text{vol}(G)}{bT} \left( \sum_{r=1}^T (P^r) \right) D^{-1} \right) \quad \text{rename argument of log as } Q \\ &= \log Q. \end{aligned}$$

Throughout this manuscript, we will refer to  $\log Q$  as the deepwalk matrix. As mentioned previously, the matrix  $M$  is ill-imposed, since pairs of nodes that never occur in  $\Omega$  lead to  $\log 0 = -\infty$ . To circumvent this computational trouble, Qiu et al [12] consider the truncated version  $M' = \log(\max(Q, 1))$  leading to a highly sparse representation. Consequently, they only consider pairs of nodes that occur in  $\Omega$  during the decomposition process, or even more dramatically, they ignore the information from most of the entries of  $M$ . netmf finally returns the matrix of node embeddings  $Y = U_d \sqrt{\Sigma_d}$ , by explicitly factorizing the closed-form of the deepwalk matrix with SVD via  $M' = U_d \Sigma_d V_d^T$ .

### 3. Methods

#### 3.1. Datasets

In our work we consider standard network datasets to study the effect of truncating or smoothing negative pairs in matrix factorization algorithms. Table 1 summarizes the basic details of these datasets. Note that, to visually demonstrate the ramifications due to the truncation of negative PMI scores, we utilize a small network of social ties among the members of a university karate club [15]. We chose this small network such that we could visually depict the shifted PMI matrices (of size  $34 \times 34$ ) when we truncate and when we smooth negative pairs (see Section 4). However, we do not use this small network for our link prediction evaluation since it would not be sufficient due to a very small sample size. In our link prediction experiments, we include 5 networks that were considered in [1]. Note that these are state of the art network datasets used for benchmarking link prediction models. A full curated list of these datasets is available from <sup>1</sup>SNAP (Stanford Large Network Dataset Collection).

| Dataset          | Type       | $ V $  | $ E $   | Description   |
|------------------|------------|--------|---------|---|
| karate club [15] | undirected | 34     | 78      | Social ties among the members of a university karate club |
| PPI [13]         | undirected | 3,852  | 38,705  | Protein-protein interaction network                       |
| ca-HepTh         | undirected | 8,638  | 24,826  | Collaboration network of Arxiv High Energy Physics        |
| ego-Facebook     | undirected | 4,039  | 88,234  | Social circles from Facebook (anonymized)                 |
| wiki-Vote        | directed   | 7,066  | 103,663 | Wikipedia who-votes-on-whom network                       |
| ca-AstroPh       | undirected | 17,903 | 197,031 | Collaboration network of Arxiv Astro Physics              |

Table 1: Datasets considered in all experiments. Note that the PPI dataset is no longer available from the SNAP website (Last checked: May 27, 2020). To use the same dataset that was tested in this work you would have to download the version available in [1]. PPI dataset was originally published in [13].

#### 3.2. Link prediction and evaluation

We perform link prediction [7] experiments in this work to compare different approaches. In essence, this type of prediction tests the quality of graph embeddings to preserve the structure; to predict the topology of the graph. In the graph embeddings community this type of intrinsic evaluation has been popularized by Grover et al. [4]. Formally, it consists in splitting graph edges  $E$  into two partitions (not necessarily of the same size)  $E_{train}, E_{test}$ , which serve the purpose of *positive* edges. Then, the non-existent edges  $(u, v) \notin E$  are sampled to make  $E_{train}^-, E_{test}^-$ , which serve as *negative* examples. Finally, graph embeddings  $Y$  are learned with algorithms trained on  $E_{train}, E_{train}^-$ , and their accuracy is evaluated on  $E_{test}, E_{test}^-$ . For the purposes of this work, we obtain graph embeddings via low-rank matrix factorization with SVD. For instance, if we rank- $d$  decompose the matrix  $M$  with SVD as  $M \approx U_d \Sigma_d V_d^T$ , then we set graph embeddings to  $Y = U_d \sqrt{\Sigma_d}$ , similar to what is done in [12]. The final classifier uses graph embeddings  $Y$  for the link prediction with  $g(Y) = \sigma(Y \cdot Y^T)$ , where  $\sigma(x) = \frac{1}{1+e^{-x}}$  is the sigmoid function. The performance of the classifier is measured with the area under the receiver-operating curve (ROC AUC). In our work we use 5-fold cross-validation, and we report average accuracy metrics. To better compare the performance due to the decomposition of different matrices, we also sometimes report a signed difference in percentage of the scores for two matrices  $M, M'$ , computed with the following function

<sup>1</sup><https://snap.stanford.edu/data/>

$$\phi(M, M') = \frac{\text{ROC AUC score}(M) - \text{ROC AUC score}(M')}{\text{ROC AUC score}(M')} \times 100.$$

### 3.3. Software used

All of our experiments were primarily implemented in Python (version 3.6). We used the usual packages from the scientific Python stack, such as numpy, scipy, and scikit-learn. To compare our approach with the NETMF algorithm, we used the <sup>2</sup>official implementation available on GitHub.

## 4. Results

### 4.1. If we truncate negatives can we properly reconstruct the PMI matrix?

We start our incursion into the effect of truncating or smoothing negatives on link prediction, by visually investigating the reconstruction of the PMI matrix. First, we apply the original netmf algorithm on the karate club network to obtain graph embeddings  $Y$ . Then we compare the ground truth PMI matrix (Figure 1, left) and its reconstruction with  $Y \cdot Y^T$  (Figure 1, right). We can see that the factorization of the truncated shifted PMI matrix  $-\log[\max(Q, 1)] = Y \cdot Y^T$  from the netmf algorithm – seriously downgrades the contribution of low-frequency pairs  $(u, v)$ , where  $Q_{uv} < 1$ . While netmf reconstruction is fairly good for highly frequent pairs of nodes, there is little variation between the non-occurring pairs and the pairs that occur with a low PMI. Consequently, the variation in low frequency pairs is squished and their contribution in the matrix factorization process via SVD is downgraded.

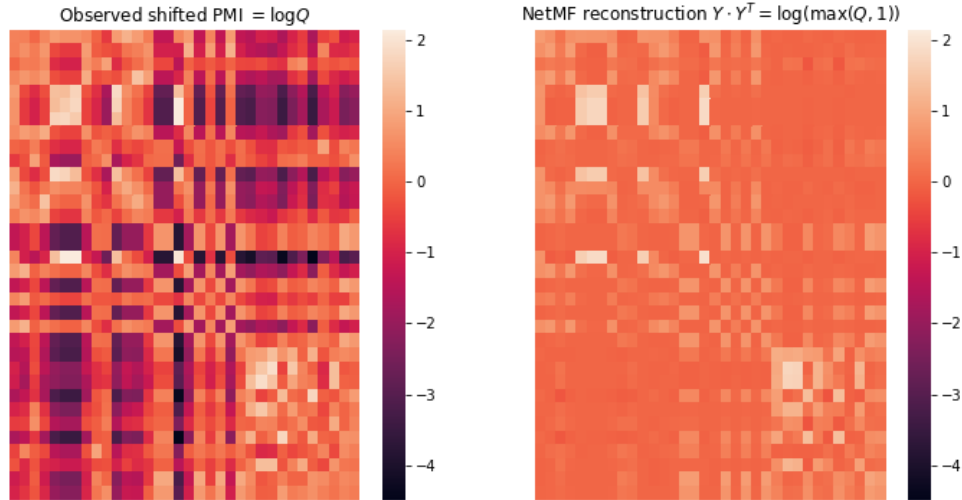


Figure 1: Left: ground truth shifted PMI matrix for the Karate graph; Right: netmf approximation. Low-rank factorization was computed with dim 5, neg size 1, window size 5. Changing hyperparameter values does not change the fact that netmf ignores low frequency pairs.

---

<sup>2</sup><https://github.com/xptree/NetMF>

#### 4.1.1. The effect of PMI matrix truncation on link prediction

Next, we measure the effect of truncating low frequency pairs on link prediction performance on larger networks. To do so, we perform a 5-fold cross-validation of the link prediction performance of the graph embeddings that we obtain by performing SVD on i)  $\log[\max(Q, 1)]$ ; the netmf algorithm, and ii)  $\sigma(\log Q)$ ; smoothened shifted PMI. For all networks we fix the hyperparameters as follows: the length of random walks is set to 10, leading to the computation of the 10-th power of the transition matrix  $P^{10}$ ; the number of negatives  $b = 10$ ; and the dimension (rank of the matrix factorization)  $d = 128$ . We smoothen the shifted PMI matrix by applying the sigmoid function  $\sigma(x) = \frac{1}{1+e^{-x}}$  element-wise. This smoothing transformation maps inputs from the  $[-\infty, \infty]$  range into the  $[0, 1]$  range. Due to this transformation the information from unobserved pairs, or the pairs with very low PMI, is not lost. However, this comes at the cost of decomposing a dense  $\sigma(\log Q)$  matrix in order to get the graph embeddings  $Y$ . Note that we cannot decompose the original shifted PMI matrix  $\log Q$ , since it leads to decomposing ill-defined  $\log 0 = -\infty$  entries. In Table 2 we present averaged ROC AUC scores on the test set when we decompose two matrices. In parenthesis, we show the increase of the average test ROC AUC score when we choose to decompose the sigmoid-smoothened version of PMI matrix, rather than the truncated PMI matrix, originally proposed by the netmf algorithm. For all considered networks the matrix decomposition of  $\sigma(\log Q)$  leads to better link prediction performance. Sometimes this increase is moderate as in the case of CA-HEPTh, a 4.48% increase from an average test ROC AUC score 0.85 to 0.89, but for other graphs the increase is more drastic. CA-ASTROPH and EGO-FACEBOOK lead to a 15+% increase, and PPI and WIKI-VOTE lead to 35+% increase, respectively. This clear improvement in link prediction performance strongly suggests that the graph embeddings obtained via SVD are extremely sensitive to the information encoded by the pairs of nodes with low PMI scores. Truncating unobserved pairs or pairs with low co-occurrence statistics may seriously downgrade the link prediction performance.

| Graph $G$<br>Matrix $M$ | ca-AstroPh           | ca-HepTh            | ego-facebook         | ppi                  | wiki-vote            |
|-------------------------|----------------------|---------------------|----------------------|----------------------|----------------------|
| $\log[\max(Q, 1)]$      | 0.85 (0.00%)         | 0.85 (0.00%)        | 0.84 (0.00%)         | 0.61 (0.00%)         | 0.66 (0.00%)         |
| $\sigma(\log Q)$        | <b>0.98 (15.15%)</b> | <b>0.89 (4.48%)</b> | <b>0.98 (16.19%)</b> | <b>0.85 (38.78%)</b> | <b>0.90 (36.74%)</b> |

Table 2: The effect of PMI matrix truncation and smoothing on link prediction for the considered networks. Averaged ROC AUC scores from a 5-fold cross-validation are reported in table cells; the difference in percent of an average test ROC AUC score of  $\sigma(\log Q)$  to the average score obtained with  $\log[\max(Q, 1)]$  is shown in parenthesis ( $\phi(\sigma(\log Q), \log[\max(Q, 1)])$ ). Best scores are shown in **bold**

#### 4.2. Matrix factorization of PMI matrix the only option for link prediction?

Inspired by the positive results induced by the  $\sigma(\cdot)$  transformation of the PMI matrix, we ask ourselves a question whether the PMI matrix should be considered the only option? The skip-gram powered neural graph embedding approaches relied on word2vec to learn latent vector representation by implicitly factorizing the shifted PMI matrix. Driven by the goal of theoretically explaining deepwalk-like neural graph embedding algorithms, Qiu et al. [12] settled for the PMI matrix, and especially its closed-form expression in graph-theoretic terms. However, the choice of the PMI matrix was implicitly imposed by the design of the neural embedding algorithm; PMI matrix was never proposed as the only solution for good node representations.

To test our hypothesis, we consider the SVD of different matrices that all represent some statistics quantity that can be computed from a graph. Table 3 gives an overview of the considered matrices, and details what one entry in each matrix means. In particular, we compare various transformations of the original PMI matrix: i)  $\log[\max(Q, 1)]$ , truncation of low frequency pairs as in netmf, ii)  $\sigma(\log Q)$ , smoothing of low frequency pairs, and iii)  $e^{\log Q}$ , the raw ratio of joint probability to the product of individual probabilities (undo the log transformation). In addition, we consider the vanilla adjacency matrix  $A$ , and the matrix  $J$  that contains joint probabilities of nodes  $i, j$  to co-occur in any random walk. We derive  $J$ 's closed-form expression in the following subsection.



| matrix $M$         | meaning of entry $M_{ij}$  |
|--------------------|--|
| $\log[\max(Q, 1)]$ | truncated shifted point-wise mutual information $\log[\max(Q_{i,j}, 1)]$ for nodes $i, j$                          |
| $\sigma(\log Q)$   | smoothened shifted point-wise mutual information $\log Q_{i,j}$ for nodes $i, j$                                   |
| $e^{\log Q}$       | undo log transformation of $\frac{p(i,j)}{p(i)p(j)}$   |
| $A$                | nodes $i, j$ are connected (1: yes, 0: no)   |
| $J$                | $P(i, j)$ - probability $p(i, j)$ that nodes $i, j$ co-occur within the same context in all simulated random walks |
| $\sigma(M)$        | $\sigma(x) = \frac{1}{1+e^{-x}}$ applied to each entry of $M$  |

Table 3: Matrices whose SVD low-rank factorization is considered in our link prediction experiments. An entry  $M_{ij}$  in a considered matrix  $M$  records a statistic of co-occurrence of two nodes  $i, j$ ; graph statistics are derived from random walks.

#### 4.2.1. Matrix form for random walk context window co-occurrence probability

Qiu et al. [12] formally show the analytic expression of the co-occurrence probability of nodes  $w, c$  in any random walk, as in

$$p(w, c) \sim \frac{\#(w, c)}{|\Omega|} \rightarrow_p \frac{1}{2T} \sum_{r=1}^T \left( \frac{d_w}{\text{vol}(G)} (P^r)_{w,c} + \frac{d_c}{\text{vol}(G)} (P^r)_{c,w} \right).$$

Herein, we derive the matrix form of this analytical expression with:

$$\begin{aligned}
J &= \frac{1}{2T} \sum_{r=1}^T \left( \frac{d_w}{\text{vol}(G)} (P^r)_{w,c} + \frac{d_c}{\text{vol}(G)} (P^r)_{c,w} \right) \\
&= \frac{1}{2T \cdot \text{vol}(G)} \left( \sum_{r=1}^T D(P^r) + \sum_{r=1}^T (P^r)^T D \right) \\
&= \frac{1}{2T \cdot \text{vol}(G)} \left( \sum_{r=1}^T \underbrace{DD^{-1}A \times D^{-1}A \times \dots \times D^{-1}A}_I + \right. \\
&\quad \left. + \sum_{r=1}^T \underbrace{AD^{-1} \times \dots \times AD^{-1}}_{r-1 \text{ times}} \times A \underbrace{D^{-1}D}_I \right) \\
&= \frac{1}{T \cdot \text{vol}(G)} \sum_{r=1}^T \underbrace{AD^{-1} \times \dots \times AD^{-1}}_{r-1 \text{ times}} \times A \\
&= \frac{1}{T \cdot \text{vol}(G)} \left( \sum_{r=1}^{T-1} (P^r)^T \right) A.
\end{aligned}$$

This matrix form of  $J$  gives us a closed-form solution for random walk co-occurrence probability computation, without the need for generating random walk sentences and sampling context pairs.

#### 4.2.2. Link prediction performance of different pairwise graph statistics

We cross-validate the link prediction performance of the graph embeddings obtained through the process of low-rank matrix factorization with SVD of the considered pairwise graph statistics. All link prediction accuracy scores on validation sets, measured with ROC AUC, are summarized in Table 4. Note that, for each matrix we report mean ROC AUC scores from 5-fold cross-validation, and the relative difference of the mean score to the mean score of the  $\log[\max(Q, 1)]$  matrix decomposition; the difference is given in signed percentages.

| Graph $G$<br>Matrix $M$ | ca-AstroPh           | ca-HepTh            | ego-facebook         | ppi                  | wiki-vote            |
|-------------------------|----------------------|---------------------|----------------------|----------------------|----------------------|
| $A$                     | 0.95 (11.04%)        | 0.85 (-0.73%)       | 0.96 (14.33%)        | 0.72 (17.15%)        | 0.75 (13.61%)        |
| $J$                     | <i>0.97 (13.67%)</i> | <i>0.89 (4.27%)</i> | <b>0.99 (17.80%)</b> | <b>0.90 (46.55%)</b> | <b>0.95 (43.52%)</b> |
| $\log[\max(Q, 1)]$      | 0.85 (0.00%)         | 0.85 (0.00%)        | 0.84 (0.00%)         | 0.61 (0.00%)         | 0.66 (0.00%)         |
| $e^{\log Q}$            | 0.62 (-27.12%)       | 0.68 (-20.73%)      | 0.83 (-0.85%)        | 0.41 (-32.52%)       | 0.63 (-5.30%)        |
| $\sigma(A)$             | 0.95 (11.33%)        | 0.85 (-0.39%)       | 0.96 (14.79%)        | 0.74 (20.56%)        | 0.74 (12.63%)        |
| $\sigma(J)$             | 0.81 (-5.41%)        | 0.72 (-16.02%)      | 0.73 (-12.66%)       | <i>0.85 (38.40%)</i> | <i>0.91 (37.66%)</i> |
| $\sigma(\log Q)$        | <b>0.98 (15.15%)</b> | <i>0.89 (4.48%)</i> | <i>0.98 (16.19%)</i> | <i>0.85 (38.78%)</i> | 0.90 (36.74%)        |
| $\sigma(e^{\log Q})$    | <b>0.98 (15.22%)</b> | <b>0.90 (4.92%)</b> | <i>0.98 (16.45%)</i> | 0.84 (37.14%)        | 0.90 (36.01%)        |

Table 4: Average test ROC AUC scores for a matrix  $M$  from a 5-fold cross-validation on all considered datasets. Improvement or deterioration of  $M$ 's score over that of the  $\log Q$  score is shown in percent in parenthesis; computed with  $\phi(M, \log[\max(Q, 1)])$ . Best link prediction accuracy results are in **bold**, second best are in *italics*.

If we consider all matrices without the  $\sigma(\cdot)$  transformation, then it is clear that the original approach of netmf is underperforming. Even the adjacency matrix, the easiest matrix to compute, can be decomposed in such a way, that the vector embeddings would perform a better link prediction than the original approach. Only the scores for the CA-HEPTh are virtually the same, for all the other graphs  $A$  improves  $Q$  by at least 11%. On the other hand,  $J$  can be decomposed in the ways that largely improve the accuracy of link prediction. We can get a 40+% increase for WIKI-VOTE and PPI graphs, 13+% increase on EGO-FACEBOOK and CA-ASTROPH, and a rather small 4+% improvement on CA-HEPTh. These results strongly indicate that the original approach is severely hindered by not learning from the variance of low-frequency pairs of nodes. This claim is further supported if we consider the  $\sigma(\cdot) \circ e$  transformation (the composition of exponentiation and sigmoid), the results look much better. Compared to  $J$ ,  $\sigma(e^{\log Q})$  is even able to have a slightly better mean test ROC AUC score on CA-ASTROPH and CA-HEPTh graphs (0.98 vs. 0.97, 0.90 vs. 0.89, respectively). The performance is slightly worse on the remaining graphs, however, it is much better than on the original  $\log[\max(Q, 1)]$  matrix. Also note that the sigmoid transformation is instrumental in the increase of performance, as simply *undoing* the log with the exponentiation operator does not improve the performance. All mean ROC AUC scores of  $e^{\log Q}$  are worse than those of the original  $\log[\max(Q, 1)]$  matrix.

In Figure 2 we show distributions of test ROC AUC score as barplots with errors in terms of one standard deviation. In general, if we compare the extent of uncertainties for one specific graph then all methods are comparable. However, we can see that the barplot is significantly wider for the original approach on the EGO-FACEBOOK graph, and slightly narrower for PPI. Notwithstanding, the mean ROC AUC score is still worse for the original approach.

#### 4.2.3. Effect of using $\sigma(\cdot)$

Next, we study the effect of applying the sigmoid transformation, element-wise for all considered matrices, on the mean ROC AUC test score. We already saw that it can dramatically increase the accuracy of the graph embeddings that rely on smoothened PMI statistics in Section 4.1.1. In the following we discuss its effect on other matrices. Recall that,  $\sigma(x) = \frac{1}{1+e^{-x}}$  squishes inputs from the  $[-\infty, \infty]$  into the  $[0, 1]$  range. Also note that  $A$  and  $J$  have their elements bounded by the  $[0, 1]$  range. Table 5 shows the effect of applying sigmoid to all considered matrices. We see that the sigmoid transformation has a tremendous positive effect on  $e^{\log Q}$  (increases of 17% - 103%) and a strongly negative effect on  $J$  (can decrease the performance by up to -25%). The effect on  $A$  is negligible. A possible explanation as to why the performance of  $J$  is so strongly hindered could be that all co-occurrence probabilities are very small positive numbers (e.g.,  $[1e-3 - 1e-1]$ ) that all get squished to an even narrower range (e.g.,  $[1e-7, 1e-5]$ ). This reduction of the range could hinder the SVD algorithm to find good vector representations.

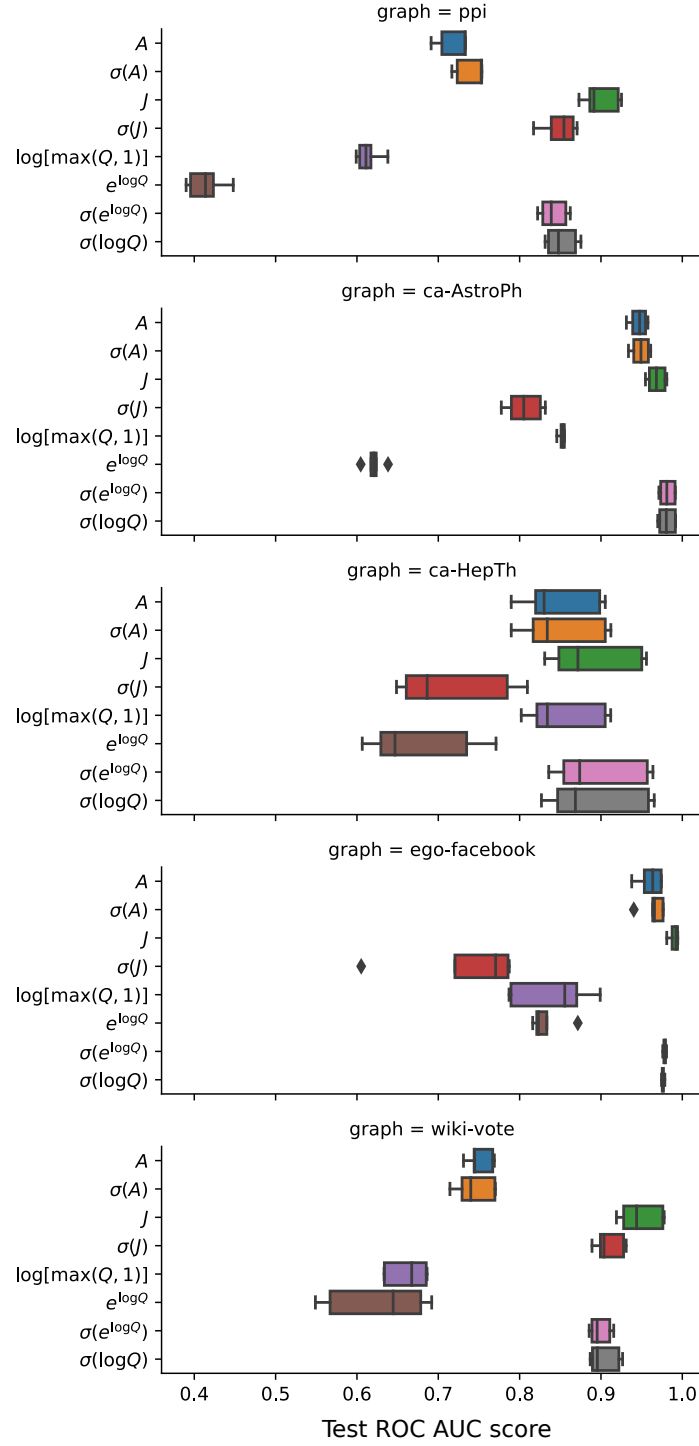


Figure 2: Average test ROC AUC scores and standard deviations, for all matrices, for all graphs.

| Graph $G$<br>Matrix $M$                       | ca-AstroPh                        | ca-HepTh                          | ego-facebook                      | ppi                               | wiki-vote                        |
|---|-----------------------------------|-----------------------------------|-----------------------------------|-----------------------------------|----------------------------------|
| $A \rightarrow \sigma(A)$                     | 0.95 $\rightarrow$ 0.95 (0.26%)   | 0.85 $\rightarrow$ 0.85 (0.34%)   | 0.96 $\rightarrow$ 0.96 (0.41%)   | 0.72 $\rightarrow$ 0.74 (2.91%)   | 0.75 $\rightarrow$ 0.74 (-0.86%) |
| $J \rightarrow \sigma(J)$                     | 0.97 $\rightarrow$ 0.81 (-16.78%) | 0.89 $\rightarrow$ 0.72 (-19.45%) | 0.99 $\rightarrow$ 0.73 (-25.86%) | 0.90 $\rightarrow$ 0.85 (-5.56%)  | 0.95 $\rightarrow$ 0.91 (-4.08%) |
| $e^{\log Q} \rightarrow \sigma(e^{\log Q})$   | 0.62 $\rightarrow$ 0.98 (58.10%)  | 0.68 $\rightarrow$ 0.90 (32.35%)  | 0.83 $\rightarrow$ 0.98 (17.45%)  | 0.41 $\rightarrow$ 0.84 (103.25%) | 0.63 $\rightarrow$ 0.90 (43.62%) |
| $\log[\max(Q, 1)] \rightarrow \sigma(\log Q)$ | 0.85 $\rightarrow$ 0.98 (15.15%)  | 0.85 $\rightarrow$ 0.89 (4.48%)   | 0.84 $\rightarrow$ 0.98 (16.19%)  | 0.61 $\rightarrow$ 0.85 (38.78%)  | 0.66 $\rightarrow$ 0.90 (36.74%) |

Table 5: The effect of using  $\sigma(\cdot)$  on average test ROC AUC scores on all considered datasets. The effect is shown by comparing the average test ROC AUC scores of a matrix  $M$  and its sigmoid transformation  $\sigma(M)$  as  $M \rightarrow \sigma(M)$ ; signed difference in percent, computed with  $\phi(\sigma(M), M)$ , is depicted in parenthesis. Note that in case of  $\log[\max(Q, 1)]$  the sigmoid transformation is applied to the untruncated matrix  $\log Q$ .

#### 4.2.4. Generalization gap

Finally, we analyze the generalization gap for all methods. We look at the average difference between the test and train ROC AUC scores. In the statistical learning theory, under the bias-variance tradeoff paradigm, we expect the test score to be slightly worse than the train score. Moreover, really big negative differences may point to the overfitting phenomenon, where a prediction model has learned the training dataset, but failed to generalize on the test set. Table 6 reports the generalization gap for all methods. Roughly speaking, all methods follow the general tendency of slightly worse test results. Surprisingly,  $e^{\log Q}$  and  $\log[\max(Q, 1)]$  perform slightly better on the test set than on the training set for the EGO-FACEBOOK graph - a positive difference of 3.91%, 4.47%, respectively. However, we can see that for some graphs the generalization gap is rather big,  $-15.76\%$  and  $-13.03\%$  for  $e^{\log Q}$ , and  $-10.86\%$  and  $-15.48\%$  for  $\log[\max(Q, 1)]$  on CA-HEPTh and ppi, respectively. This points to a strong overfitting. For the same graphs,  $A$ 's gaps are  $-10.53\%$  and  $-12.95\%$ , and  $J$ 's gaps are  $-9.96\%$  and  $-8.29\%$ , respectively. For all other graphs, the gaps of  $A$  and  $J$  stay under  $-3\%$ , and the gaps of  $\log[\max(Q, 1)]$  stay under  $-7\%$ . The sigmoid smoothening  $\sigma(\log Q)$  of PMI drastically improves the accuracy, however, this comes at a stronger generalization gap wrt.  $J$  on PPI graph ( $-13.65\%$  vs.  $-8.29\%$ ), and on WIKI-VOTE ( $-7.24\%$  vs  $3.50\%$ ).

| Graph $G$<br>Matrix $M$ | ca-AstroPh   | ca-HepTh   | ego-facebook                                       | ppi  | wiki-vote  |
|-------------------------|--|--|--|--|--|
| $A$                     | $0.97 \rightarrow 0.95$ (-2.80%)                   | $0.95 \rightarrow 0.85$ (-10.53%)                  | $0.97 \rightarrow 0.96$ (-0.70%)                   | $0.83 \rightarrow 0.72$ (-12.95%)                  | $0.73 \rightarrow 0.75$ (3.16%)                    |
| $J$                     | $0.99 \rightarrow 0.97$ (-1.93%)                   | $0.99 \rightarrow 0.89$ (-9.96%)                   | <b><math>1.00 \rightarrow 0.99</math> (-0.63%)</b> | <b><math>0.98 \rightarrow 0.90</math> (-8.29%)</b> | <b><math>0.98 \rightarrow 0.95</math> (-3.50%)</b> |
| $\log[\max(Q, 1)]$      | $0.87 \rightarrow 0.85$ (-2.48%)                   | $0.96 \rightarrow 0.85$ (-10.86%)                  | $0.80 \rightarrow 0.84$ (4.47%)                    | $0.73 \rightarrow 0.61$ (-15.48%)                  | $0.71 \rightarrow 0.66$ (-6.95%)                   |
| $\sigma(\log Q)$        | $1.00 \rightarrow 0.98$ (-1.52%)                   | $0.99 \rightarrow 0.89$ (-9.65%)                   | $0.98 \rightarrow 0.98$ (-0.40%)                   | $0.99 \rightarrow 0.85$ (-13.65%)                  | $0.97 \rightarrow 0.90$ (-7.24%)                   |
| $e^{\log Q}$            | $0.65 \rightarrow 0.62$ (-4.41%)                   | $0.80 \rightarrow 0.68$ (-15.76%)                  | $0.80 \rightarrow 0.83$ (3.91%)                    | $0.48 \rightarrow 0.41$ (-13.03%)                  | $0.66 \rightarrow 0.63$ (-4.59%)                   |
| $\sigma(A)$             | $0.98 \rightarrow 0.95$ (-2.85%)                   | $0.96 \rightarrow 0.85$ (-10.87%)                  | $0.97 \rightarrow 0.96$ (-1.02%)                   | $0.84 \rightarrow 0.74$ (-12.37%)                  | $0.73 \rightarrow 0.74$ (2.13%)                    |
| $\sigma(J)$             | $0.84 \rightarrow 0.81$ (-3.62%)                   | $0.81 \rightarrow 0.72$ (-10.93%)                  | $0.80 \rightarrow 0.73$ (-8.01%)                   | $0.87 \rightarrow 0.85$ (-2.92%)                   | $0.93 \rightarrow 0.91$ (-1.88%)                   |
| $\sigma(e^{\log Q})$    | <b><math>1.00 \rightarrow 0.98</math> (-1.45%)</b> | <b><math>0.99 \rightarrow 0.90</math> (-9.31%)</b> | $0.98 \rightarrow 0.98$ (-0.40%)                   | $0.98 \rightarrow 0.84$ (-14.39%)                  | $0.97 \rightarrow 0.90$ (-7.11%)                   |

Table 6: Generalization gap between an average test ( $X_{test}$ ) and train ( $X_{train}$ ) ROC AUC scores for a matrix  $M$ ; depicted as  $X_{test} \rightarrow X_{train}$ ; signed difference in percent, computed with  $\phi(X_{test}, X_{train})$  in parenthesis. Big positive difference points to overfitting. A good generalization gap is determined as the highest test ROC AUC score, with moderately small generalization gap. Best generalization gaps are in **bold**, second-best in *italics*.

#### 4.2.5. Comparison with state-of-the-art neural graph embeddings

Finally, we compare the obtained link prediction scores with those reported in [1] (Table 7). In [1] the authors used a neural graph embedding model that was implicitly factorizing the expected values of the matrix of co-occurrence counts  $\mathbb{E}[C]$ , where each entry  $C_{wc}$  represents the expected amount of times  $\mathbb{E}[\#(w, c)]$  that nodes  $w, c$  will co-occur in all random walks. This work detains the state-of-the-art link prediction scores on the same datasets used in this work, outperforming other neural graph embedding algorithms. Our approach based on explicit matrix factorization via SVD obtains comparable scores.

| Graph $G$<br>Matrix $M$ | ca-AstroPh  | ca-HepTh    | ego-facebook | ppi         | wiki-vote   |
|-------------------------|-------------|-------------|--------------|-------------|-------------|
| $J$                     | 0.97        | 0.89        | <b>0.99</b>  | <b>0.90</b> | <b>0.95</b> |
| $\sigma(\log Q)$        | <b>0.98</b> | 0.89        | <i>0.98</i>  | 0.85        | 0.90        |
| $\sigma(e^{\log Q})$    | <b>0.98</b> | <i>0.90</i> | <i>0.98</i>  | 0.84        | 0.90        |
| $\mathbb{E}[C]^\dagger$ | <b>0.98</b> | <b>0.93</b> | <b>0.99</b>  | <b>0.91</b> | <i>0.93</i> |

Table 7: Comparison of test ROC AUC scores from the best performing matrices in this work to the scores obtained with a state-of-the-art neural graph embedding algorithm [1].  $^\dagger$  scores are copy-pasted from [1], their algorithm was not tested on exactly the same splits used in our experiments. Best scores gaps are in **bold**, second-best in *italics*.

## 5. Discussion

### 5.1. Truncate or smoothen negatives?

From our results, there is a strong signal that  $\log[\max(Q, 1)]$  should not be considered as a good matrix for link prediction problems. Mainly, because all the variation in low-frequency pairs joint probabilities is flattened by the  $\max(\cdot, 1)$  transformation. In fact, the  $\sigma(\cdot)$  transformation of the PMI matrix  $\sigma(\log Q)$  yields a much better link prediction performance, since all the variance of the low-frequency pairs – most entries in the graph co-occurrence statistics matrix – is taken into account during the matrix factorization with the SVD. Therefore, smoothening *negatives* should be favored to *truncating* them for link prediction.

### 5.2. Should we only limit ourselves to the low-rank decomposition of the PMI matrix?

All matrices whose decomposition we considered in this work represent quantities derived from the co-occurrence frequencies in simulated random walks – akin to what the PMI matrix is measuring; the adjacency matrix  $A$  could be considered as such matrix where random walks are limited to 1 step forward. In our experiments, we saw that the accuracy of link prediction of the graph embeddings obtained via low-rank matrix factorization with SVD strongly depend on which transformations we perform to these graph co-occurrence statistics. For instance, while the  $e^{\log Q}$  leads to poor link prediction results, its sigmoid transformation  $\sigma(e^{\log Q})$  yields impressive boost in accuracy, from an increase of +17 to +103%, depending on the dataset.

While the smoothened version of the PMI matrix  $\sigma(\log Q)$  yielded among the best link prediction scores for some graphs, it was outperformed by other matrices for other graphs. In particular, the joint probability matrix  $J$ , whose matrix form we derived in this work, has demonstrated either the best or among the best link prediction accuracy scores for all graphs. But why  $J$  should outperform other PMI-based matrices, if all of them encode co-occurrence information from the same graph and for the same simulated random walks? We believe that to explain this, we need to analyze under which circumstances a relatively high joint probability of  $i$  and  $j$  appearing together encodes more useful information for link prediction problem. Point-wise mutual information of a pair of outcomes  $x, y$  from discrete random variables  $X$  and  $Y$  quantifies the discrepancy between the probability of their coincidence (co-occurrence) given their joint distribution and their individual distributions. In computational linguistics, PMI is used for finding collocations and associations between words. Good collocation pairs have high PMI because the probability of co-occurrence  $p(i, j)$  is only slightly lower than the probabilities of occurrence of each word ( $p(i)$  and  $p(j)$ ). On the other hand,  $\text{PMI}(i, j)$  is zero when these two outcomes are independent, i.e.,  $p(i, j) = p(i)p(j)$ ;  $\text{PMI}(i, j) = \log \left[ \frac{p(i, j)}{p(i)p(j)} \right] = \log 1 = 0$ . And it is undefined when  $i, j$  do not co-occur at all, i.e., if  $p(i, j) = 0$  then  $\log \text{PMI}(i, j) = \log \left[ \frac{p(i, j)}{p(i)p(j)} \right] = \log 0 = -\infty$ . On the other hand, PMI is maximized when two outcomes are perfectly associated, i.e.,  $p(i|j) = 1$  or  $p(j|i) = 1$ . For instance, a pair of words PUERTO RICO has a very high PMI, since they are rarely used individually in the <sup>3</sup>Wikipedia articles. From the same source, a pair of words IT THE, despite having the same joint probability value as PUERTO RICO, will have a very low PMI score, because their joint probability is small in comparison with their individual probabilities.

Translating to the graph domain, consider two connected nodes  $i, j$ , such that both  $i$  and  $j$  are extremely frequent (very high centrality). If we compute the PMI of this pair it will give us a very low score, because the numerator (joint probability) is dominated by the denominator (big individual probabilities), therefore the dot product of embeddings for these two nodes will give us a low score, which might be interpreted that the two nodes are not connected (while they are). This can seriously undermine the link predictor. Therefore, we believe that a high joint probability for two highly frequent nodes should not be penalized, as it might be very indicative of a very plausible link between the two nodes. Hence, we would recommend  $J$ , the joint probability matrix, as the main choice for the computation of node embeddings for link prediction.

---

<sup>3</sup>[https://en.wikipedia.org/wiki/Pointwise\\_mutual\\_information](https://en.wikipedia.org/wiki/Pointwise_mutual_information)

### 5.3. Neural graph embeddings or matrix factorization?

Even though our results are on par with the state-of-the-art link prediction performance achieved by a neural graph embedding model, it was not the main goal to contrast neural embeddings with the embeddings obtained via matrix factorization, and determine the absolute best. Rather, we believe that certain points could be valuable for a more focused comparison, that one could extract from our work. Neural embeddings are intended to learn embeddings in an end-to-end manner, by extracting the necessary structure from the raw input data. Yet, in the case of deepwalk and other methods based on random walks simulation, the input is pre-processed in such a manner that a neural network automatically decomposes a matrix, whose entries encode co-occurrence information from random walks. In other words, the matrix to decompose is implicitly imposed. One of the difficulties with neural embeddings approaches is the hyperparameter optimization. How to find the right rank  $d$  (embedding dimension), how to find the right amount of negatives  $b$  in the case of SGNS loss? These and many other parameters have to be determined empirically, which adds up to the computational complexity. On the other hand, the Eckart-Young-Mirsky theorem gives us guarantees that the SVD decomposition of a matrix will be the best  $d$ -rank linear decomposition. In other words, if we stick to a specific rank choice (embedding dimension) we can be sure that the decomposed vectors are the best linear approximation. Whereas, in the case of neural embeddings there is no such guarantee. Notwithstanding, neural embeddings may extract non-linear patterns, and therefore learn even better node embeddings, with a possibly smaller rank. The biggest assumption of matrix factorization models is that the target matrix can be decomposed linearly, which may not always be the case.

However, if we shift focus from linear vs. non-linear, as was already demonstrated in [6, 12, 1] the interplay between neural networks and matrix factorization is intertwined. At least for the symbolic data, such as words and nodes in a graph. This suggests that the advancement of the state of the art in one may be utilized in the other. For example, the fact that the joint probability may be a better candidate for matrix factorization for link prediction may be exploited by neural embedding models, i.e., learning embeddings that factorize the joint probability matrix rather than the PMI matrix. In addition, a matrix factorization approach can be used as a baseline model during the process of training more complex neural embedding models.

### 5.4. Related work

Our work is based on the tremendous previous efforts to connect neural embeddings for symbolic data and the solid theory of matrix factorization [6, 12]. Perhaps, the most similar work to ours, to the best of our knowledge, comes from the NLP domain [5], where they showed that the SVD decomposition of the truncated PMI matrix, as in [6], may worsen the quality of word embeddings.

### 5.5. Limitations

Our analysis is heavily tied to the linear low-rank decomposition assumption of the SVD algorithm. It is not excluded that, another matrix factorization algorithm could have decomposed the truncated  $\log[\max(Q, 1)]$  matrix in such a way as to learn better node embeddings for link prediction. However, it would be surprising that the information coming from only high-frequency pairs would be sufficient for the link prediction in different graphs with different structure. On another note, the original netmf [12] was not tested on link prediction problems, meaning that the factorization of the truncated PMI was not initially proposed as a good candidate for link prediction. The authors compared  $\log[\max(Q, 1)]$  decomposition with deepwalk (and related approaches) on node classification problems. Lastly, our proposition of smoothening the information coming from low-frequency pairs might yield a highly dense matrix; our approach might not scale as well as the original approach in [12], which emphasized sparsification via truncation  $\log[\max(Q, 1)]$ .

### 5.6. Conclusion

In this work, we pushed forward our understanding of the interplay between the skip-gram powered neural graph embedding algorithms and the matrix factorization via SVD. Neural graph embeddings implicitly decompose matrices that represent quantities derived from the co-occurrence frequencies in simulated random walks. Using explicit matrix factorization approaches via SVD we can obtain graph embeddings

of rank  $d$  with guarantees of best possible linear decomposition for this rank; alleviating thus the pain of hyperparameter tuning for the correct graph embedding  $d$ , under the linear decomposition assumption. We showed that the link prediction accuracy of graph embeddings strongly depends on the transformations of the original graph co-occurrence matrix that they decompose. Point-wise mutual information matrix need not be the only option, and if it is, then the entries corresponding to low-frequency pairs should be smoothened and not truncated for a better performance on link prediction.

## References

- [1] S. Abu-El-Haija, B. Perozzi, R. Al-Rfou, and A. A. Alemi. Watch your step: Learning node embeddings via graph attention. In S. Bengio, H. Wallach, H. Larochelle, K. Grauman, N. Cesa-Bianchi, and R. Garnett, editors, *Advances in Neural Information Processing Systems 31*, pages 9180–9190. Curran Associates, Inc., 2018.
- [2] F. R. K. Chung. *Spectral Graph Theory*. American Mathematical Society, 1997.
- [3] Y. Goldberg and O. Levy. word2vec explained: deriving mikolov et al.’s negative-sampling word-embedding method, 2014.
- [4] A. Grover and J. Leskovec. Node2vec: Scalable feature learning for networks. In *Proceedings of the 22nd ACM SIGKDD International Conference on Knowledge Discovery and Data Mining*, page 855–864, 2016.
- [5] K. Kenyon-Dean. Word embedding algorithms as generalized low rank models and their canonical form, 2019.
- [6] O. Levy and Y. Goldberg. Neural word embedding as implicit matrix factorization. In *Proc. NIPS*, page 2177–2185, 2014.
- [7] D. Liben-Nowell and J. Kleinberg. The link prediction problem for social networks. In *Proceedings of the twelfth international conference on Information and knowledge management - CIKM '03*, page 556, New York, New York, USA, nov 2003. ACM Press.
- [8] L. Lovász. Random walks on graphs: A survey. In D. Miklós, V. T. Sós, and T. Szőnyi, editors, *Combinatorics, Paul Erdős is Eighty*, volume 2, pages 353–398. János Bolyai Mathematical Society, Budapest, 1996.
- [9] T. Mikolov, K. Chen, G. Corrado, and J. Dean. Efficient estimation of word representations in vector space, 2013.
- [10] T. Mikolov, I. Sutskever, K. Chen, G. Corrado, and J. Dean. Distributed representations of words and phrases and their compositionality. *arXiv*, oct 2013.
- [11] B. Perozzi, R. Al-Rfou, and S. Skiena. Deepwalk: Online learning of social representations. In *Proceedings of the 20th ACM SIGKDD international conference on Knowledge discovery and data mining - KDD '14*, pages 701–710, New York, New York, USA, aug 2014. ACM Press.
- [12] J. Qiu, Y. Dong, H. Ma, J. Li, K. Wang, and J. Tang. Network embedding as matrix factorization: Unifying deepwalk, line, pte, and node2vec. In *Proc. WSDM*, page 459–467, 2018.
- [13] C. Stark, B.-J. Breitkreutz, T. Reguly, L. Boucher, A. Breitkreutz, and M. Tyers. BioGRID: a general repository for interaction datasets. *Nucleic Acids Research*, 34:D535–D539, 01 2006.
- [14] L. Tang and H. Liu. Relational learning via latent social dimensions. In *Proceedings of the 15th ACM SIGKDD International Conference on Knowledge Discovery and Data Mining*, page 817–826, New York, NY, USA, 2009. Association for Computing Machinery.
- [15] W. W. Zachary. An information flow model for conflict and fission in small groups. *Journal of anthropological research*, pages 452–473, 1977.